COMMUNICATIONS IN NUMERICAL METHODS IN ENGINEERING
Commun. Numer. Meth. Engng. 2000; **16**:257–266

A quadratic boundary element implementation in orthotropic elasticity using the real variable approach

G. S. Padhi, R. A. Shenoi, S. S. J. Moy* and G. L. Hawkins

Computational Engineering and Design Centre, Faculty of Engineering and Applied Science, University of Southampton, Highfield, Southampton, SO17 1BJ, U.K.

SUMMARY

This paper revisits the real variable fundamental solution approach to the Boundary Integral Equation (BIE) method in two-dimensional orthotropic elasticity. The numerical implementation was carried out using quadratic isoparametric elements. The strong and weakly singular integrals were directly evaluated using Euler's transformation technique. The limiting process was done in intrinsic coordinates and no separate numerical treatment for strong and weak singular integrals was necessary. For strongly singular integrals *a priori* interpretation of the Cauchy principal value is not necessary. Two problems from plane stress and strain are presented to demonstrate the numerical efficiency of the approach. Excellent agreement between BEM results and exact solutions was obtained even with relatively coarse mesh discretizations. Copyright © 2000 John Wiley & Sons, Ltd.

KEY WORDS: boundary element method; orthotropic elasticity; real variable approach; direct evaluation; Euler's transformation technique

1. INTRODUCTION

Boundary Integral Equation (BIE) techniques are well established in solving boundary value problems. An important feature of the BIE method is that instead of attempting to find an approximate solution for the governing differential equation throughout the relevant solution domain, the governing equation is converted into an integral form, often involving only integrals over the boundary of the solution domain. Consequently, only the boundary has to be discretized in order to carry out the integrations. The dimensionality of the problem is effectively reduced by one: a three-dimensional volume problem becomes a two-dimensional surface problem, and so on. Also, because the interior of a solution domain is not discretized, there is less approximation involved in representing the solution variables.

The literature available on BIE implementation for isotropic elasticity is extensive [1–3]. Comparatively recently, various approaches to the numerical implementation of BIE in anisotropic elasticity have been reported. Broadly they can be grouped into two categories. In the first, the

*Correspondence to: S. S. J. Moy, Department of Civil and Environmental Engineering, University of Southampton, Highfield, Southampton S017 1BJ, U.K.

Received 9 February 1998
Accepted 20 September 1999

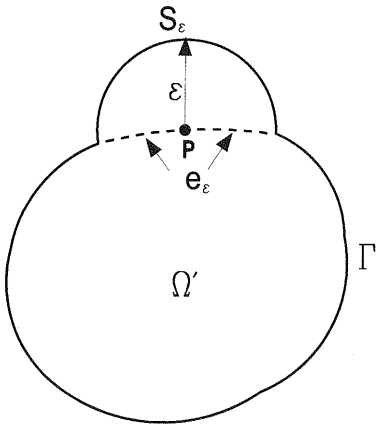

Figure 1. Exclusion of the singular point P by a vanishing neighbourhood S_ε.

isotropic fundamental solution (Kelvin's solution) is still used, resulting in a volume integral term associated with the anisotropy of the material, which is numerically treated by discretizing the domain into internal cells [4]. In the second category, anisotropic fundamental solutions similar to Kelvin's solution for isotropic elasticity are used. These can be based on functions of either the real or the complex variable.

Rizzo and Shippy [5] first used the two-dimensional anisotropic fundamental solution presented by Green [6] in a real variable formulation. Constant elements were used to model the geometry and approximate the field variables. Mahajerin and Sikarskie [7] used BIE based on real variables, with constant elements, for calculating stress concentration factors in double-lap joints. Vable *et al.* [8] and Benjumea *et al.* [9] reported further applications of the real variable approaches. Snyder and Cruse [10] were the first to use the complex variable anisotropic fundamental solution. This spurred further work based on the complex variable fundamental solutions [4, 11–13]. From the literature review it is clear that, the few papers which have reported on the numerical implementation of BIE based on real variables have, at best, used line elements.

As far as the evaluation of singular integrals in BEM is concerned, the earliest approach for calculating the strongly singular integrals has been the use of the rigid-body motion technique [14] that indirectly gives the sum of these integrals and the free term coefficients. Another approach has been to regularize the singular integral equations in which the strength of the highest singularity is reduced by order one. The literature available on regularization techniques is too extensive to discuss here. For weakly singular integrals, numerical techniques, including special weighted quadratures and mapping methods have been reported in the literature. Tanaka *et al.* [15] have summarized the regularization procedures for both singular and hypersingular integral equations that have appeared in literature and therefore no attempt is made here to discuss these techniques. It is evident that mathematical similarity often exists in these techniques. In a series of papers, Guiggiani *et al.* [16–19] have tried to evaluate the strongly singular and hypersingular integrals directly. In these papers the original boundary is recast with an exclusion zone e_ε and a spherical boundary bump S_ε (Figure 1). Integration over S_ε is performed analytically, independent of discretization. For calculating the limit of the integral over $\Gamma - e_\varepsilon$, the exclusion zone is mapped on to the intrinsic co-ordinate space and the singular integrands are expanded into Laurent series about the singular

point. The singular integrals in the series expansion are evaluated analytically with canceling of the divergent terms, and the limit is taken.

The purpose of this paper is to report on an application of the BIE implementation for orthotropic elasticity with potential application for complex problems in laminated plates and structures. This has been achieved by: (a) computation of weak and strong singular integrals using a unified integration module based on Euler's transformation technique; (b) applying this approach to typical plane stress and strain problems; (c) assessing the numerical efficiency of the new approach using constant, linear and quadratic elements.

2. THE BIE METHOD FOR PLANE ORTHOTROPIC ELASTICITY

The development of the boundary element method for orthotropic materials under plane stress follows the same steps as in isotropic elasticity [1–3]. It is based on unit load solutions in an infinite body, known as the fundamental solutions. Use of these with the Betti–Rayleigh reciprocal work theorem and carrying out the appropriate mathematical limiting operations results in the BIE for the displacements at an interior point p due to tractions and displacements on the surface at a boundary point Q. In the absence of body forces it can be written as

$$u_k(p) + \int_\Gamma T_{kl}(p,Q)u_k(Q)\,\mathrm{d}\Gamma(Q) = \int_\Gamma U_{kl}(p,Q)t_k(Q)\,\mathrm{d}\Gamma(Q) \tag{1}$$

where $u_k(p)$ are the displacements in the x_k directions at the interior point p, $u_k(Q)$ and $t_k(Q)$ are the displacements and tractions respectively at the boundary point Q. The kernel functions U_{kl} and T_{kl} are unit load solutions in an infinite domain. For 2-D orthotropic elasticity, explicit expressions for the kernel functions, based purely on real variables can be found in Rizzo and Shippy [5], following earlier work by Green [6]. It is well known that the first integral in Equation (1) has $1/r$ singularity and the second integral has $\log 1/r$ singularity when p approaches the boundary of the domain.

Because of the singular nature of the fundamental solutions, Equation (1) has to be set up in a limiting form to obtain the boundary integral equation suitable for numerical implementation. Assuming the body can be represented as shown in Figure 1 with the point P (which is really a boundary point) as an internal point surrounded by part of a spherical surface S_ε of radius ε, Equation (1) can be written as

$$u_k(P) + \int_{\Gamma - e_\varepsilon + S_\varepsilon} T_{kl}(P,Q)u_k(Q)\,\mathrm{d}\Gamma(Q) = \int_{\Gamma - e_\varepsilon + S_\varepsilon} U_{kl}(P,Q)t_k(Q)\,\mathrm{d}\Gamma(Q) \tag{2}$$

As discussed in References [16, 17], the surrounding zone S_ε need not be a spherical surface. To arrive at the boundary integral equation, the limit of Equation (2) has to be found as $\varepsilon \to 0$. If the integrals in Equation (2) are broken into summation of integrals over the regions $\Gamma - e_\varepsilon$ and S_ε and their limits as $\lim_{\varepsilon \to 0}$ are studied, it can be shown that the limit quantity which often needs special treatment is

$$I = \lim_{\varepsilon \to 0} \int_{\Gamma - e_\varepsilon} T_{kl}(P,Q)u_k(Q)\,\mathrm{d}\Gamma(Q) \tag{3}$$

As usual if a boundary element discretization procedure is adopted, both the integrand and the limiting process have to be translated from the Euclidean space into the intrinsic co-ordinate (ξ)

space. This translation procedure can be found in Guiggiani's works [16, 17]. In the case of the singular point P belonging to two quadratic boundary elements, the corresponding exclusion zones for them can be denoted as e_ε^1 and e_ε^2. These zones can be mapped onto the intrinsic co-ordinate space. Denoting their lengths in the intrinsic co-ordinate space as $\alpha_1(\varepsilon)$ and $\alpha_2(\varepsilon)$, the final form of Equation (3) in the intrinsic co-ordinate space can be written as

$$I = \lim_{\varepsilon \to 0} \left\{ \int_{-1+\alpha_2(\varepsilon)}^{1} T_{ij}(-1,\xi) N_c(\xi) J(\xi)\, \mathrm{d}\xi + \int_{-1}^{1-\alpha_1(\varepsilon)} T_{ij}(1,\xi) N_c(\xi) J(\xi)\, \mathrm{d}\xi \right\} \tag{4}$$

where $J(\xi)$ is the Jacobian. The quantities $\alpha_m(\varepsilon)$ can be expanded in a Taylor series in terms of ε as

$$\alpha_m(\varepsilon) = \varepsilon \beta_m(\eta) + 0(\varepsilon^2) \tag{5}$$

where $m = 1, 2$, and $\beta_m(\eta) = 1/J^m(\eta)$ and $\eta = 1$ for $m = 1$, $\eta = -1$ for $m = 2$.

As shown by Guiggiani [16, 17], since the singularities are of order $1/r$, only one term is required in the Taylor series expansion.

Returning back to Equation (2), it can be easily observed that the other limit integral with a singular kernel is

$$I = \lim_{\varepsilon \to 0} \int_{\Gamma - e_\varepsilon} U_{kl}(P,Q) t_k(Q)\, \mathrm{d}\Gamma(Q) \tag{6}$$

Since the fundamental solution U_{kl} has logarithmic (weak) singularity when the source point P approaches the field point, the integral exists in the ordinary Riemann sense even though the integrand is not defined at the singular point. However because of the singular nature, numerical evaluation of these integrals often needs special treatment. In this work these integrals have been treated similarly to the strongly singular integrals from a computational point of view. Hence, the integral in Equation (6) can be written in the intrinsic co-ordinate space as

$$I = \lim_{\varepsilon \to 0} \left\{ \int_{-1+\alpha_2(\varepsilon)}^{1} U_{ij}(-1,\xi) N_c(\xi) J(\xi)\, \mathrm{d}\xi + \int_{-1}^{1-\alpha_1(\varepsilon)} U_{ij}(1,\xi) N_c(\xi) J(\xi)\, \mathrm{d}\xi \right\} \tag{7}$$

3. DIRECT NUMERICAL EVALUATION OF THE LIMIT

The approach for evaluating the limit is the same for Equations (4) and (7). The procedure for evaluating the limit in the strongly singular case, Equation (4), is outlined below. The limiting integral is evaluated using Euler's transformation technique as follows. Even though the individual integrands on the right-hand side of Equation (4) are not defined at $\varepsilon = 0$, the integral quantity I exists and can be evaluated without evaluating the integrands at the singular point.

A sequence of values of ε decreasing in magnitude and approaching but not equal to zero are chosen. These values can be represented as $\varepsilon_0, \varepsilon_1, \varepsilon_2, \ldots, \varepsilon_n$ and the corresponding finite integral values can be represented as $I_0, I_1, I_2, \ldots, I_n$. The limit of this sequence, $\lim_{n \to \infty} I_n$, is the desired quantity, and is calculated as follows. If a new sequence is formed as

$$I_1 - I_0, I_2 - I_1, \ldots, I_n - I_{n-1} \tag{8}$$

then

$$\lim_{n\to\infty} I_n = I_0 + \lim_{n\to\infty} (I_1 - I_0 + I_2 - I_1 + \cdots + I_n - I_{n-1}) \tag{9}$$

The second part of the right-hand side can be approximated from n difference quantities using Euler's transformation technique (see the appendix) which gives an infinite sum through finite sampling as

$$\lim_{n\to\infty} (I_1 - I_0 + I_2 - I_1 + \cdots + I_n - I_{n-1}) = \text{EulerSum}\ (I_1 - I_0 + I_2 - I_1 + \cdots + I_n - I_{n-1}) \tag{10}$$

Once the approximated infinite sum is calculated, it is back substituted into Equation (9) and the limiting value of the integral is found.

4. COMPUTER IMPLEMENTATION

The above algorithm for obtaining the limit of a function has been implemented in the symbolic computer program *Mathematica 3.0* [20] as a standard AddOn Package. The corresponding function is NLimit. All the limit integrals are evaluated directly using the Euler's transformation technique. No unbounded terms arise when the singular point P is taken to the boundary, since the

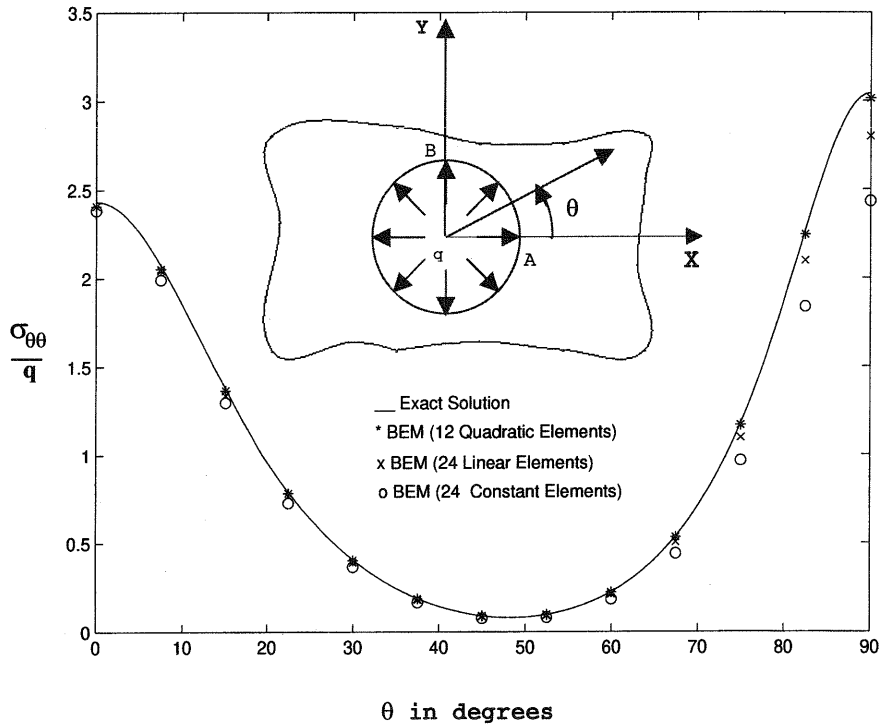

Figure 2. Normalized tangential stress at the hole boundary (infinite plate with a circular hole subjected to hydrostatic pressure).

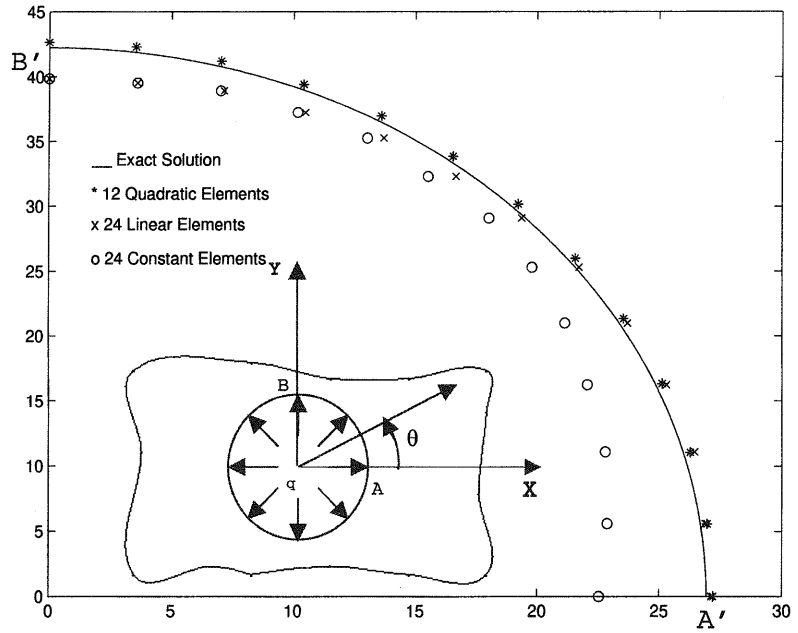

Figure 3. Deformed shape of one-quarter of the inner boundary with unit radius (infinite plate with a circular hole) subjected to hydrostatic pressure).

unbounded divergent terms cancel each other out. The implementation of Euler's transformation technique for finding an infinite sum makes no assumptions regarding the strength of singularity or dimensionality of the problem. Therefore, it can be extended to more complicated 3-D and hyper-singular formulations. The number of finite terms to choose in the Euler's transformation technique depends on rate of convergence of the function for which the limit is to be evaluated. In the present analysis, five terms were satisfactory.

The computing work was done on a Silicon Graphics Work Station running under Irix 6.0 operating system with an 195 MHz IP28 Iris processor with 128 Mbytes of main memory.

5. ILLUSTRATIONS

Two examples are presented for illustration purposes. In each case three different element types, constant, linear and quadratic, have been studied for comparison purposes. In each problem, the number of nodes was kept constant for the three element types, to give a realistic comparison of numerical efficiencies. No units have been chosen but any consistent set could be used. The stresses tangential to the boundary have been determined by differentiation of the shape functions and use of the constitutive equations.

Example 1 deals with an infinite plate with a circular hole, at the boundary of which uniform hydrostatic pressure is applied (Figure 2). The material properties are: $E_x = 1.2$; $E_y = 0.6$; $G_{xy} = 0.7$; $v_{xy} = 0.071$.

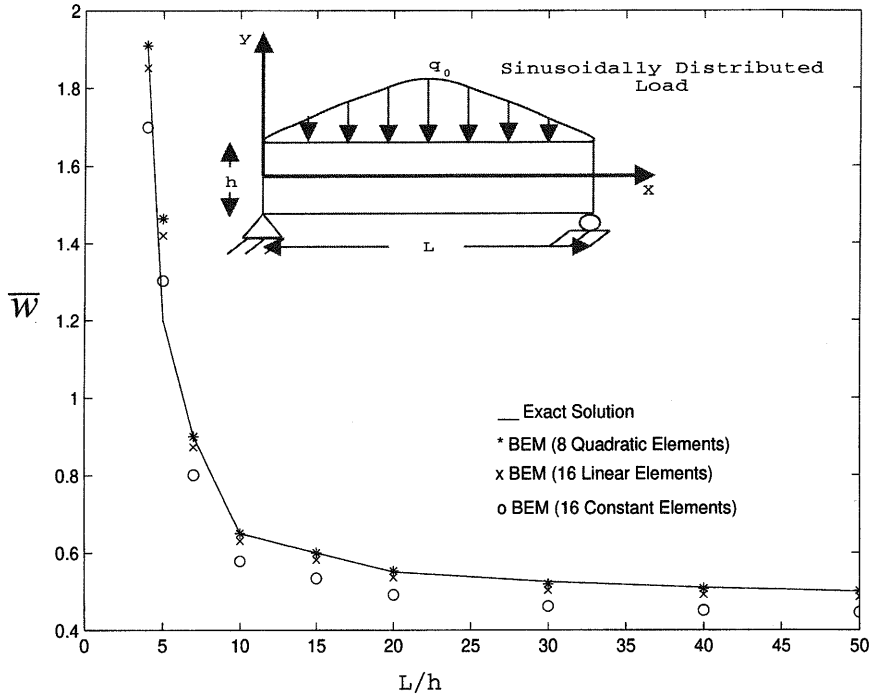

Figure 4. Normalized maximum deflection vs length/span ratio (infinitely long plate under sinusoidally distributed load).

The problem was solved using 12 quadratic boundary elements along the hole boundary. Following usual boundary element discretization, since the domain is infinite, the node numbering was done in reverse (clockwise) direction. To compare the numerical efficiency of the present approach with the results presented in the literature, the same problem was solved with 24 linear and 24 constant elements.

Figure 2 compares the numerical results for hoop stress ($\sigma_{\theta\theta}$) with analytical results due to Lekhntiskii [21]. The error was less than 0.5 per cent using quadratic elements, about 3 per cent with linear elements and more than 10 per cent with constant elements. It may be noted that although accurate results were obtained by Rizzo and Shippy [5], considerably more nodes were used (24 nodes for one quarter of the hole). Figure 3 compares the deformed shape of one quarter of the hole boundary (of unit radius) obtained using quadratic, linear and constant elements with the exact elliptical one [21]. A′ and B′ represent the deformed positions of the corresponding points A and B on the hole boundary. The average errors are 0.5, 3 and 10 per cent respectively.

Example 2 considers an infinitely long (in the z direction) orthotropic plate simply supported along the long edges ($x=0$, $x=L$) and subjected to sinusoidally distributed load at the top surface of the form $q(x)=q_0 \sin(\pi x/L)$. It was assumed to be under plane strain condition.

The material parameters for this problem were: $E_x=25\times10^6$; $E_y=E_z=10^6$; $G_{xy}=G_{xz}=0.5\times10^6$; $G_{yz}=10^6$; $\nu_{xy}=\nu_{xz}=\nu_{yz}=0.25$.

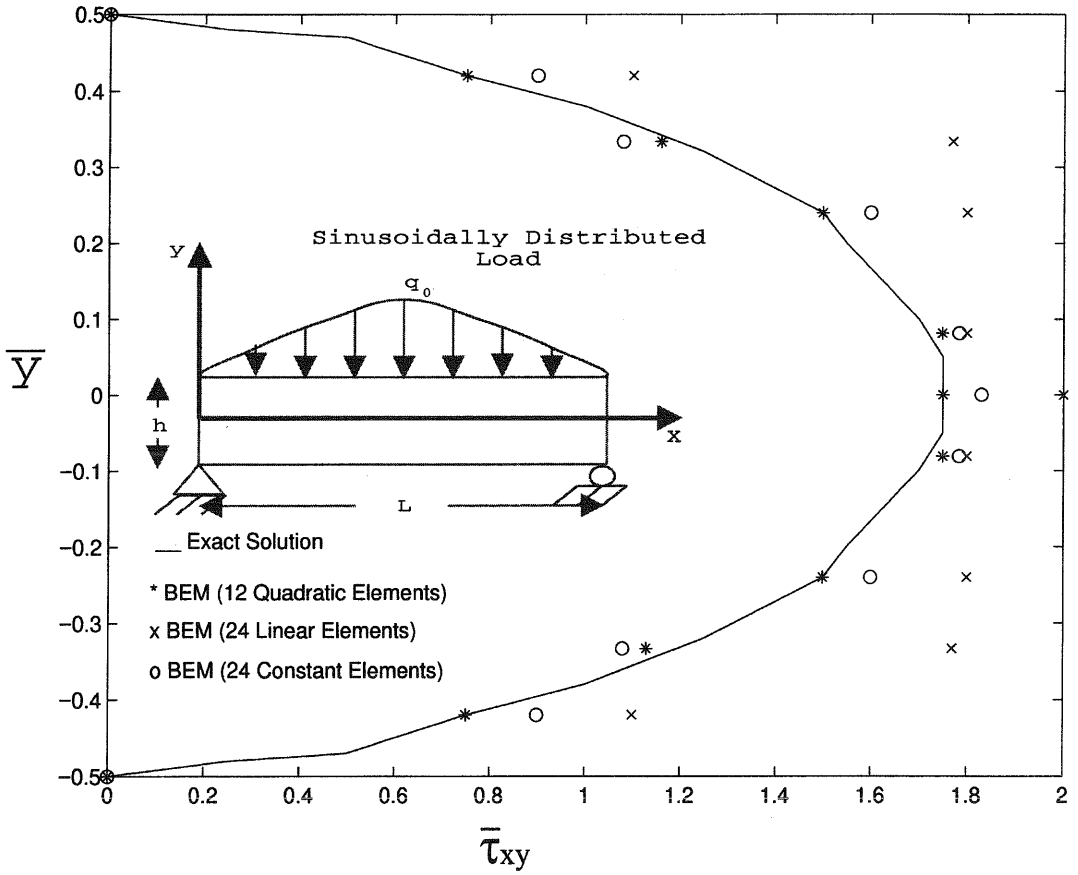

Figure 5. Normalized transverse shear stress distribution at $L/h = 4$ (infinitely long plate under sinusoidally distributed load).

To compare the present results with Pagano's 3-D elasticity solution [22] the stresses and displacements were normalized in the form

$$\bar{w} = \frac{100E_y h^3 w(L/2, 0)}{q_0 L^4}; \quad \bar{y} = \frac{y}{h} \quad \text{and} \quad \bar{\tau}_{xy} = \frac{\tau_{xy}(0, y)}{q_0} \tag{11}$$

where w is the maximum central deflection, h is the plate thickness and q_0 is the maximum amplitude of the sinusoidally distributed load at the top surface. This problem was solved using eight quadratic elements for aspect ratio $L/h = 4$, although more elements were added for higher aspect ratios.

Figure 4 compares the normalized maximum deflection obtained by the present approach using quadratic, linear and constant elements with the results given by the 3-D elasticity solution [22] for different L/h ratios. The present BEM results with quadratic elements closely followed the elasticity solution, less than 0.5 per cent error, while linear and constant elements gave errors 3 and 10 per cent, respectively.

Figure 5 presents the normalized shear stress across the depth of the plate, numerical solution had an error of less than 0.5 per cent with quadratic elements. The constant elements were more accurate (error 10 per cent) than the linear ones (error 25 per cent).

6. CLOSURE

In this paper Euler's transformation technique has been successfully used to calculate the limits of various integrals occurring when the general BIE method in orthotropic elasticity based purely on real variables is numerically implemented using quadratic boundary elements. Two problems from plane stress and strain were solved to demonstrate the numerical efficiency of the present approach. A comparative study has been made of the BIE procedure using constant, linear and quadratic elements in the discretization. For problems involving bending, in which a rapidly varying traction field is prescribed as the boundary condition, it was found that both constant and linear elements gave highly inaccurate results, while the error with quadratic elements was less than 1 per cent.

APPENDIX: SUMMATION OF AN INFINITE SERIES VIA FINITE SAMPLING USING EULER'S TRANSFORMATION TECHNIQUE

Given any series

$$S = a_0 + a_1 + a_2 + a_3 + \cdots + a_{n-1} + a_n + \cdots \tag{A1}$$

define $x = a_n/a_{n-1}$, so that the series can be re-written as

$$S = a_0 + x\frac{a_1}{x} + x^2\frac{a_2}{x^2} + x^3\frac{a_3}{x^3} + \cdots + x^{n-1}\frac{a_{n-1}}{x^{n-1}} + x^n\frac{a_n}{x^n} + \cdots \tag{A2}$$

where n is the number of finite terms used to give an approximation to the infinite sum. The series can be re-written as

$$S = u_0 + u_1 x + u_2 x^2 + \cdots \tag{A3}$$

where $u_0 = a_0$, $u_1 = a_1/x$, $u_2 = a_2/x^2$ and so on. Using the relationships $Eu_0 = u_1$, $E^2u_0 = u_2$, $E^3u_0 = u_3 \ldots$, then symbolically

$$S = (1 + Ex + E^2x^2 + \cdots)u_0 = \frac{1}{1 - Ex}u_0 \tag{A4}$$

where E is a shift operator such that $Ef(x) = f(x+h)$ and h is the interval length. Using $E = \Delta + 1$, Equation (A4) can be re-written as

$$S = \frac{u_0}{1 - x - x\Delta} = \frac{1}{1 - x}\left(\frac{u_0}{(1 - (x/(1 - x))\Delta)}\right) \tag{A5}$$

where Δ is the difference operator such that $\Delta f(x) = f(x+h) - f(x)$, or $\Delta u_0 = u_1 - u_0$, $\Delta^2 u_0 = u_2 - 2u_1 + u_0$, etc.

The summation formula in Equation (A5) can now be re-written as

$$S = \frac{1}{1-x} \times \sum_{s=0}^{\infty} \left(\frac{x}{1-x} \right)^s \Delta^s u_0 \tag{A6}$$

Using the difference quantities in the terms of the original sequence, Equation (A6) can be re-written as

$$S = \frac{1}{1-x} \times \sum_{s=0}^{\infty} \left(\frac{1}{1-x} \right)^s \Delta^s a_0 \tag{A7}$$

This is Euler's transformation of the original series which is found to converge faster than the original series. It is not necessary to sum to infinity in Equation (A6); it will be sufficiently accurate to use a finite number of terms (say, p), thus requiring the first p differences obtained from the terms starting at u_0.

REFERENCES

1. Brebbia CA, Telles JCF, Wrobel LC. *Boundary Element Techniques.* Springer-Verlag: Berlin, 1984.
2. Becker AA. *The Boundary Element Method in Engineering.* McGraw-Hill: London, 1992.
3. Rizzo FJ. An integral equation approach to boundary value problems of classical elastostatics. *Quarterly Journal of Applied Mathematics* 1967; **25**:83–95.
4. Perez MM, Wrobel LC. An integral equation formulation for anisotropic elastostatics. *ASME Journal of Applied Mechanics* 1996; **63**:891–902.
5. Rizzo FJ, Shippy DJ. A method for stress determination in plane anisotropic body. *Journal of Composite Materials* 1970; **4**:36–61.
6. Green AE. A note on stress systems in aelotropic materials. *Philosophical Magazine* 1943; **34**:416–418.
7. Mahajerin E, Sikarskie DL. Boundary element study of a loaded hole in an orthotropic plate. *Journal of Composite Materials* 1986; **20**:375–389.
8. Vable M, Sikarskie DL. Stress analysis in plane orthotropic material by the boundary element method. *International Journal of Solids and Structures* 1988; **24**:1–11.
9. Benjumea R, Sikarskie DL. On the solution of plane orthotropic elasticity problems by an integral method. *ASME Journal of Applied Mechanics* 1972; **39**:801–808.
10. Snyder MD, Cruse TA. Boundary integral equation analysis of cracked anisotropic plates. *International Journal of Fracture* 1975; **11**:315–328.
11. Tan CL, Gao YL, Afagh FF. Anisotropic stress analysis of inclusion problems using the boundary integral equation. *Journal of Strain Analysis* 1992; **27**:67–76.
12. Tan CL, Gao YL. Boundary element analysis of plane anisotropic bodies with stress concentration and cracks. *Journal of Composite Structures* 1992; **20**:17–28.
13. Lee KJ, Mal AK. A boundary element method for plane anisotropic elastic media. *ASME Journal of Applied Mechanics* 1990; **57**:600–606.
14. Rizzo FJ, Shippy DJ. An advanced boundary integral method for three dimensional elasticity. *International Journal for Numerical Methods in Engineering* 1977; **1**:1753–1768.
15. Tanaka M, Sladek V, Sladek J. Regularization techniques applied to boundary element methods. *ASME Applied Mechanical Review* 1994; **47**(10):457–489.
16. Guiggiani M, Krishnasamy G, Rudolphi TJ, Rizzo FJ. A general algorithm for the numerical solution of hypersingular boundary integral equations. *ASME Journal of Applied Mechanics* 1992; **59**:604–614.
17. Guiggiani M. Hypersingular formulation for boundary stress evaluation. Engineering Analysis with Boundary Element 1994; **13**:169–179.
18. Guiggiani M, Casalini P. Direct computation of Cauchy principal value integrals in advanced boundary elements. *International Journal for Numerical Methods in Engineering* 1987; **24**:1711–1720.
19. Guiggiani M, Gigante A. A general algorithm for multi-dimensional Cauchy principal value integrals in the boundary element method. *ASME Journal of Applied Mechanics* 1990; **57**:906–915.
20. Wolfram S. *Mathematica, A System for Doing Mathematics by Computer.* Addison-Wesley: RedWood City, CA, 1991.
21. Lekhntiskii SG. *Theory of Elasticity of an Anisotropic Elastic Body.* Holden-Day: San Francisco, 1963.
22. Pagano NJ. Exact solutions for composite laminates in cylindrical bending. *Journal of Composite Materials* 1969; **3**:398–411.

